Exploring and Applying Liquid Crystals in New Geometries Prepared by Microfluidics and Electrospinning

Hsin-Ling Liang[1,2], JungHyun Noh[3], Minsik Hwang[3], Dae Kyom Kim[3], Eva Enz[2], Per Rudquist[4] and Jan Lagerwall[3,5,*]

[1] *Johannes Gutenberg-Universität Mainz, Institute of Organic Chemistry, 55099 Mainz, Germany*
[2] *Martin-Luther-Universität Halle-Wittenberg, Institute of Chemistry - Physical Chemistry, 06120 Halle, Germany*
[3] *Seoul National University, Graduate School of Convergence Science & Technology, Department of Nanoscience & Technology, 443-270, Suwon, Korea*
[4] *Chalmers University of Technology, Department for Microtechnology and Nanoscience, 412 96 Göteborg, Sweden*
[5] *Advanced Institutes of Convergence Technologies, 443-270, Suwon, Korea*

Using a nested capillary microfluidics set-up we produce and investigate thin shells of liquid crystal (LC), suspended in aqueous host phases, focusing in particular on the structure formation of smectic phases and the behaviour at transitions between different LC phases in shell geometry. The various arrangements of topological defects and other geometrical features developing by self-assembly in these shells, and the possibility of tuning the result by modifying boundary conditions, LC phase, thickness and diameter of the shell, or by adding defect-seeding particles, make this new LC configuration very attractive. We also use coaxial electrospinning to prepare composite fibres with a core of LC (nematics or smectics, chiral or non-chiral) inside a polymer sheath. The encapsulated LC provides novel functionality and responsiveness to the composite fibres, giving them wide application possibility for instance in wearable sensors, whereas the confinement imposed by the polymer sheath can have strong impact on the behaviour of the liquid crystal. We briefly discuss the application potential, but our main focus here is on the response of the liquid crystal to the narrow cylindrical confinement inside the fibres.

Key words: liquid crystals; polymer fibres; colloids; microfluidics; electrospinning.

1. Introduction

Traditionally, liquid crystals are studied primarily in flat geometry samples. This is convenient, since it allows easy optical characterisation in e.g. a polarising microscope and since flat samples with well defined thickness and a variety of alignment agents can be manufactured relatively easily. It is also the natural choice in research related to the most common application of thermotropic liquid crystals

*jan.lagerwall@lcsoftmatter.com

Phil. Trans. R. Soc. A 1–26; doi: 10.1098/rspa.XXXXXXXX
Received 26 June 2012; Accepted ...

in flat panel displays. By restricting the study to flat samples one however imposes certain constraints on the liquid crystal, which may or may not be beneficial. Most important, the lack of curvature forbids any net topological defect in the director field; the sample is either defect-free (as is the goal in displays) or it contains positive as well as negative-signed defects, balanced such that the defect sum is zero. The latter situation has been the focus of considerable attention over the last few years, due to a series of beautiful experiments by a number of groups where colloidal inclusions seed positive topological defects, forcing the liquid crystal to create a perfectly cancelling set of negative-signed defects [1–32].

In a curved sample, in contrast, a non-zero defect sum is not just allowed, it is in fact required by topology if the director is in the curving plane. This allows for some very interesting phenomena occurring at curved liquid crystal surfaces and proposals have been made how these could be exploited in technological applications [33]. The simplest and most studied curved liquid crystal surface is that of a sphere, and liquid crystal droplets have been studied quite extensively by e.g. Kleman and Lavrentovich [34–36]. More advanced and introduced more recently is the liquid crystal shell (neglecting the soap bubble, which is probably the longest studied liquid crystal of all, at least on a child's or amateur's level), which can now be produced reliably using a microfluidics-based method [37]. The shells are typically studied as a colloidal system, with the liquid crystal shell suspended in an aqueous continuous phase, often also with the same or different aqueous mixture forming an internal droplet. Compared to full droplets the shell offers some interesting unique aspects. First, the presence of an inner as well as an outer interface gives an excellent control handle for tuning the director arrangement within the shell, since we can independently and quite easily choose between planar and homeotropic alignment, with varying anchoring strength, at the two boundaries. Moreover, by varying the size of the inner droplet we can tune the shell thickness, and very interesting effects related to an asymmetric placement of the inner drop may also occur [37]. Finally, we have considerable freedom in choosing the inner fluid and its constituents, and via osmosis-driven flow through the liquid crystal it is even possible to expand or compress the inner droplet [38], thereby affecting the shell thickness and diameter dynamically, also after shell production.

This paper focuses primarily on liquid crystal shells, discussing briefly how they are produced, which interesting physical phenomena we may encounter when studying liquid crystal shells of different types—possibly doped with nano- or microparticles—and how the unique properties of the spherical liquid crystal shell could be exploited technologically. For a deeper discussion of the general issues, considering also liquid crystal drops, we refer the interested reader to an excellent review by Fernandez-Nieves and Lopez-Leon [39]. The emphasis of the present paper lies on the authors' own work, in particular on the transition between nematic and smectic order under varying alignment combinations, and on the behaviour of SmC shells.

In addition to the shells, we briefly consider another new type of liquid crystal sample that also involves a strongly curved boundary. In this case the liquid crystal is encapsulated inside a polymer fibre with diameter in the micro- or sub-micrometer range, produced by means of electrospinning. While we generally do not have the same freedom to simply choose the director anchoring geometry at the interface in this case, we have a different flexibility in the shape of the

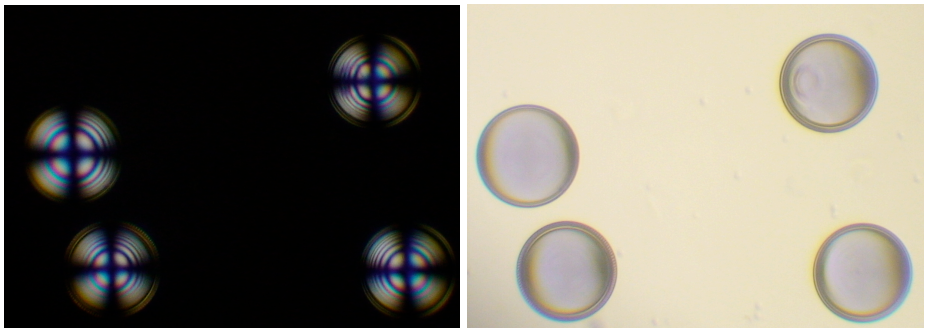

Figure 1. A series of homeotropically aligned SmA shells (about 150 μm in diameter) observed between crossed polarisers (left) and without analyser (right).

liquid crystal volume; depending on spinning conditions and choice of materials we can span the range from a quasi-infinitely long cylindrical column of liquid crystal, to break-up into droplets that may be more or less elongated in the fibre direction. In both cases the diameter can be very thin. This configuration for studying liquid crystals is interesting for several reasons. First, it constitutes a very simple, versatile and low-cost way of investigating strong confinement effects on liquid crystals, allowing characterisation by standard methods like polarising optical microscopy, x-ray scattering and differential scanning calorimetry. Second, because the concept brings the functionality of liquid crystals to polymer fibre mats this opens new avenues for applications, e.g. in smart and responsive textiles or in novel sensing devices.

2. Liquid crystal shells

(*a*) *Motivation: why study liquid crystalline shells and particles in them?*

Depending on the boundary conditions, diameter, thickness and the type of phase a liquid crystal shell can display a very rich set of textures, often quite beautiful, giving both intellectual stimulation and possible applications. The former aspect refers to the types of defect and their arrangement that can be expected and produced, respectively, in liquid crystal shells. With homeotropic anchoring on both sides the shell is defect-free and the standard appearance of such a shell resembles a conoscopy picture of a flat homeotropic uniaxial liquid crystal, cf Fig.1. By considering the optics of the two situations this resemblance is easy to understand: while conoscopy probes all light directions through a flat sample, the homeotropic aligned shell observed in orthoscopy provides all sample film orientations for a single direction of light propagation, yielding analogous results.

More interesting situations arise when at least one interface is planar-aligned. Topology tells us that a planar director field cannot be defect free on a spherical surface, or on any other surface with the same topology as a sphere for that matter (for instance an ellipsoid or even a tube with closed ends). Specifically, the defects

on the planar-aligned side(s) of the shell must be of such type and number that when their strengths are summed up, taking the sign into account, the total is s=2. The simplest configuration to imagine is one with two s=+1 defects, analogous to the defects in the meridional field at the north and south poles of the earth. In case of planar alignment on both sides of the shell an integer defect may however also split up into two $s = +1/2$ defects. It was early on proposed that the energy minimising configuration of such a shell in general would be a tetrahedral set of four $s = +1/2$ defects [33], because the energy density of a defect scales as s^2 and in a tetrahedral arrangement the distortion of the director field between the defects is minimised. When the first experiments on nematic shells were performed by Fernandez-Nieves and co-workers [37] it was realised, however, that several combinations of defects could be stable, with four, two or even three defects distributed over the shell surface. Even for the case of four $s = +1/2$ defects in the shell these are typically not in a tetrahedral configuration because the non-zero thickness of the shell and the consequent extension of the defect line between the inner and outer surfaces drives the defects towards the thinnest side of the shell. Although the energy related to the director field distortion between the defects is increased in this way, this is outweighed by the gain in energy from reducing the defect line extension. In a careful and elegant study by Lopez-Leon and co-workers [38], where the shell thickness was thinned in a controlled way by driving liquid into the inner droplet from the outer phase by osmosis, the authors concluded that different regimes can be identified, each of which has a specific number of defects in a specific configuration. For very thin shells the originally predicted, and most desired, configuration of four $s = +1/2$ defects in tetrahedral arrangement can be stabilised.

The reason that the tetrahedral arrangement of four defects is particularly attractive is that shells with this defect configuration have potential for a new type of colloidal particle, which can lead to colloidal crystallization with diamond-like symmetry [33], of particular interest for the generation of photonic crystals [40, 41] since it can produce polarisation independent complete 3D band gap. Such a colloidal crystal is very difficult to achieve by conventional means, because colloidal particles without directed interactions typically crystallize with simple cubic lattice. Defects in the nematic director field are high energy points where the mesogens are forced locally into a state not corresponding to thermodynamic equilibrium. If a polymer molecule that is not mesogenic but miscible with the liquid crystal is introduced, it will preferentially segregate towards regions of low order parameter where it can maximise its own configurational entropy [42]. The ideal location ought to be the defect, where it gains full configurational freedom and at the same time fills the volume that constitutes the high-energy point for the mesogens, reducing the system's free energy. In this way it should be possible to anchor an appropriately designed molecule, for instance a block copolymer with a random coil non-polar block miscible with the liquid crystal connected to a polar block that extends out into the aqueous continuous phase, at the defects. If the polar block is given a linking and bond-forming capacity, e.g. by using complementary single-stranded DNA (ssDNA), we would effectively have created a colloidal particle that bonds in directions dictated by the defect arrangement. If the tetragonal arrangement can be ensured we would have the carbon-like bonding

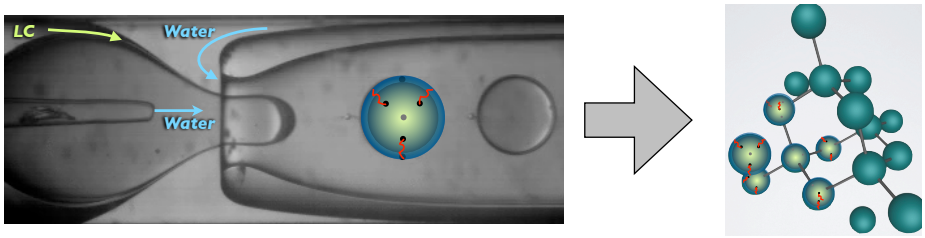

Figure 2. Graphical illustration of the concept for using liquid crystal shells functionalised by linker molecules to realise colloidal particles that can self-assemble into colloidal crystals with diamond-like symmetry. This illustration was previously used in the review article [43].

that would be needed to generate a colloidal crystal with diamond symmetry, cf. the scheme in Fig. 2.

An interesting opportunity to further tune the defect number and configuration that has not yet been explored is the deliberate addition of particles, which themselves seed defects, in the shell. Since the defect sum by topology is fixed at $s = 2$, regardless of what defects are seeded, an interesting situation would for instance arise in case of three spherical particles added to the shell, each coated as to induce an $s = +1$ defect. In order to maintain the required defect sum the liquid crystal would thus have to create an $s = -1$ defect (or perhaps a 'saturn ring' defect, effectively giving two $s = -1/2$ defects in the sample plane), and it would then have a total of four defects but only one which is not filled by a particle (for now not considering the saturn ring solution). Whereas the pristine liquid crystal shell, if thin enough and complemented with the appropriate linker molecules, would give us a colloid with 'valence' 4, this situation could give us a valence 1 situation, since only one defect is available for occupation by the linker molecule. This is a route that may be very interesting to explore for the future, since different colloid valences would open the door to a very interesting 'colloid chemistry', but we are still quite far from being able to explore this route in full since up to now no attempts have been made to actually realise the required linker molecule. The corresponding study of defect formation in particle-containing shells can however be done already now and eventually a very rich research field may emerge.

An aspect that one must keep in mind when analysing liquid crystal shells optically is that *both* shell sides contribute to the birefringence. Thus, even if the back or front side is out of focus, it will change the interference colours and it may ruin extinction if the directors on the two sides are not co-planar. This can render a proper optical analysis of a shell very difficult since the choice of outer and inner aqueous phases generally allows us to choose between planar and homeotropic alignment, but there is no way at present to further influence the director field in a planar shell in the former case. In an unlucky situation the director orientations at front and back may be close to perpendicular, rendering polarising microscopy analysis of the director field difficult. The best situation is one where either the back or front director is more or less uniform, such that

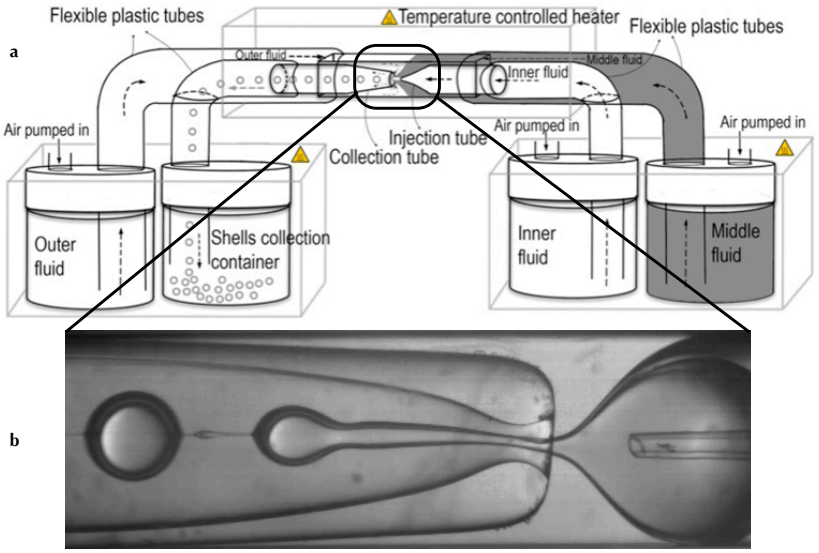

Figure 3. Scheme of the microfluidic liquid crystall shell production set-up (top) together with a high-speed video frame showing the process in reality. This illustration was previously used in the article [45].

either the polariser or analyser can be oriented in the same direction, minimising the influence of the shell side currently not in focus.

(*b*) *Shell production and stabilisation*

In our work we use a microfluidic set-up with nested glass capillaries with square and circular cross sections, respectively, designed along the principles described by Utada et al. in [44]. The outer diameter of the cylindrical capillaries is identical to the inner side length of the square capillary, such that two cylindrical capillaries can be inserted into the square one from each side, the tight fit ensuring coaxial alignment. One of the cylindrical capillaries has a tapered end, the other one a blunt end, and the two ends are placed in the near vicinity of each other at the centre of the square capillary. In order to prepare the shells the inner aqueous phase is pumped through the tapered capillary while the liquid crystal is pumped in the same direction in the square capillary, thus flowing in the corner voids surrounding the cylindrical capillary. From the other side of the square capillary the outer aqueous phase (the continuous phase) is flowed in the opposite direction, such that it meets the liquid crystal at the location where the two capillary ends meet. Because the liquid crystal is not miscible with the outer aqueous phase, both phases are flow focused into the blunt-ended cylindrical capillary which acts as collection tube. At the same time the inner aqueous phase is injected drop wise within the liquid crystal flow as the Rayleigh instability breaks up the initial stream of the two co-flowing fluids, such that shells of well-defined dimensions are produced. Fig. 3 shows a schematic drawing of the set-up together with an example micrograph of how the shell production looks in practice.

For driving the fluid flow the most common choice is to load the different fluids into syringes and use syringe pumps for pumping them into the capillaries, connected to the syringes via flexible tubing. In our case we prefer to use a computer-controlled pneumatic-based microfluidic flow control unit (Fluigent MFCS) that can pump up to 4 fluids independently. The advantage is that we need not use syringes but we can work with any vial of our choice, rendering temperature control of the different fluids much easier. We close each vial with a septum into which we insert two thin polymer tubes. One is connected to the MFCS unit, with the other end being in the air in the vial, above the fluid surface. The other tube is inserted long enough into the vial that its one end is immersed in the fluid, the other end being connected to the capillary within which this fluid should be flown. By pumping air at carefully controlled pressure into the vial through the first tube the MFCS unit pressurizes the vial such that liquid starts flowing out through the other tube and into the capillary. This construction allows for very dynamic flow control, with the response to a change in pump pressure and the stabilisation of the flow at the new speed being dramatically faster than when using syringe pumps.

In order to stabilise the shells from rupture the two aqueous phases must contain either a surfactant or a polymer that will adsorb at the water-liquid crystal interface. We use standard surfactants such as anionic sodium dodecyl sulfate (SDS), cationic cetyl trimethylammonium bromide (CTAB) or nonionic Pluronics F-127, or water soluble polymers such as polyvinylalcohol (PVA). The choice of stabiliser is of key importance because it does not just stabilise the interface, it also generally determines which alignment is adopted by the liquid crystal at that interface. SDS and CTAB induce homeotropic alignment as the non-polar alkyl chain of the surfactant extends more or less radially into the liquid crystal phase, with the ionic head group facing the aqueous phase. If planar alignment is desired, the typical choice is PVA, which most likely adsorbs at the interface albeit primarily within the aqueous phase, in a random coil conformation. This stabilises the interface and prevents shell rupture but due to the disordered polymer chain it does not necessarily have a strong impact on the liquid crystal alignment. The resulting planar alignment is instead probably a result of the contact with the polar water phase, which is known to induce planar alignment [46]. The Pluronics surfactant has turned out to be compatible with planar as well as homeotropic alignment, with opposite results for nematic and smectic phases [45].

(*c*) *Nematic-Smectic-A transition in shells with planar and hybrid boundary conditions*

We have extensively investigated the transition between nematic and smectic order in shell geometry using 8CB as the liquid crystal material, having either PVA in inner as well as outer phases to induce stable fully planar alignment [47], F-127 in both phases to induce an alignment change at the phase transition [45], or a combination of SDS or similar surfactants in one aqueous phase and PVA in the other, in order to induce hybrid alignment [48]. The first of these situations was investigated in detail also by Lopez-Leon et al. [49]. Here we very briefly summarise the main observations and conclusions, referring to the cited papers for the details.

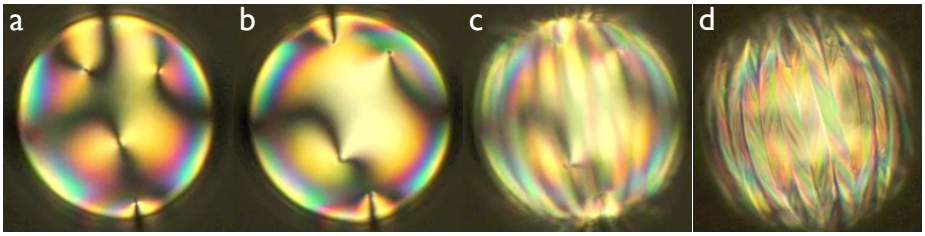

Figure 4. Nematic-Smectic-A transition on cooling an 8CB shell (about 100 μm diameter and about 4 μm thickness) with planar alignment at both interfaces. The photos were taken deep in the nematic phase (a), just before the N-SmA transition (b), just after the transition (c), and about a minute after the transition (d). Photos (a)-(c) are focused on the thinner back side of the shell, where all four director field defects are located, whereas photo (d) is focused on the thicker front side of the shell (this has been rescaled slightly to fit the frame of the other photos, since the different focus gives a larger appearance in the photo).

In case of PVA-induced fully planar alignment we typically get four $s = 1/2$ defects for reasonably thin shells but, as explained above, they are frequently not in the tetrahedral configuration but instead collected close the thinnest part of the shell in order to minimise the extension of the defect lines. Typically they are not symmetrically spaced but often roughly on a rhombus, with two defects spaced apart from each other about twice the distance of that of the other two. Fig. 4a shows a less common case where three defects are close to the thinnest part of the shell and the fourth is further away. A careful analysis of the director field around the defects led to the conclusion that the more strongly separated defects are surrounded by a director field that is primarily bent, whereas the other two are connect to mainly splay in the director field [47]. The consequent difference in energy penalty between bend and splay deformations (the former roughly twice that of the latter) makes the difference in separation understandable: by placing the costly bend defects close to each other, thereby minimising the extension through the shell of their defect lines the shell can keep the energy minimised, although this means that the splay defects will have longer defect line extensions. The lower energy density of this defect type compensates for the length increase.

On approaching the transition to smectic order all defects move away from each other, cf. Fig. 4b, an observation that may have different origins. On the one hand the increasing elastic constants on approaching smectic order would strengthen the repulsion between defects, on the other hand the shell asymmetry may be reduced somewhat on approaching the smectic phase. In support of the latter effect is the fact that both defect pairs separate while it is only the bend and twist constants K_2 and K_3 that diverge on approaching the phase transition, while the splay constant K_1 is not so much affected. On the other hand, the divergence of K_3 requires *all* defects in a fully developed smectic-A state to be pure splay defects in order to ensure stability, a situation that only occurs when all defects lie on a great circle [50]. As the phase transition is approached the defects indeed move as to adopt this configuration [47, 49].

When the shell enters the SmA phase a quite complex sequence of textural development starts. Immediately at the start of the transition a break-up of the

texture into spherical lune sections takes place on the thicker defect-free side of the shell, cf. Fig. 4c and d. The former picture is taken at the transition but the focus is on the thin side, allowing the lunes to be distinguished only by their contours. The second photo is taken about a minute later, now with focus on the thick side of the shell, giving a detailed view of the lunes. Here one can see also a secondary modulation in the texture with stripes in a herring-bone-like arrangement, reversing their inclination between adjacent lunes. This finer modulation starts slightly later than the break-up into lunes [47]. We have proposed as explanation for these textural features that a smectic layer undulation occurs in the SmA phase, with increasing magnitude going from the in- to the outside of the shell. This leads to a continuously increasing "effective" layer spacing as measured along the original director orientation, thereby making the SmA phase compatible with the increasing spherical surface area on going from the shell's inside to its outside, cf. [47] for a detailed discussion of the process. The stripes occurring as a secondary modulation can most likely be understood as another layer buckling instability, resolving a source of layer strain that arises as a result of the initial layer undulation (again, we refer to [47] for the details).

The N-SmA transition in a fully homeotropic shell, with the director firmly anchored in the radial direction on the in- as well as outside by traditional homeotropic-inducing surfactants in both aqueous phases, is not particularly interesting since both phases are fully compatible with the shell configuration with this alignment. Both phases acquire the characteristic conoscopy-like texture seen on the left in Fig. 1, the phase transition being detected only by a reduction in thermal fluctuations. More interesting was the case when the nonionic polymeric surfactant Pluronics F-127 was used in both interior and exterior phases to stabilise 8CB shells [45]. In this case the nematic phase is fully planar aligned, but as the shell is cooled towards the smectic phase the texture slowly changes, beginning with a twisted spiral-like distortion of the conoscopy cross, concurrent with the appearance of two $s = +1$ defects at top and bottom of the shell, and ending with a SmA texture that is similar to the above described spherical lune texture. The origin of this alignment change is not yet clear and further experiments are on-going to elucidate it in more detail. At present we hypothesise that the driving force is the asymmetry of the shell, resulting from the imperfect density matching of inner fluid and liquid crystal. In the nematic phase there is no problem of having different shell thickness at different points of the shell since there is no positional order in the phase, but in case of smectic order this variation is connected to a substantial energy penalty. There are then many layers present at the thickest point of the shell which are not closed up since fewer and fewer of them fit in the shell as it gets increasingly thinner towards the opposite side. Because F-127 has only a weak impact on the alignment the liquid crystal then apparently rearranges its structure entirely from homeotropic to planar alignment on approaching the smectic phase. In shells with strong homeotropic anchoring on both sides, induced e.g. by ionic surfactants like SDS or CTAB, we instead see evidence of the shell asymmetry being reduced on approaching the phase transition, with the inner drop being moved somewhat towards the shell centre (publication in preparation).

Another very interesting situation occurs if we enforce opposing alignment at the inner and outer surfaces, by using PVA in one aqueous phase and an ionic surfactant in the other. We studied a series of shells constituting various

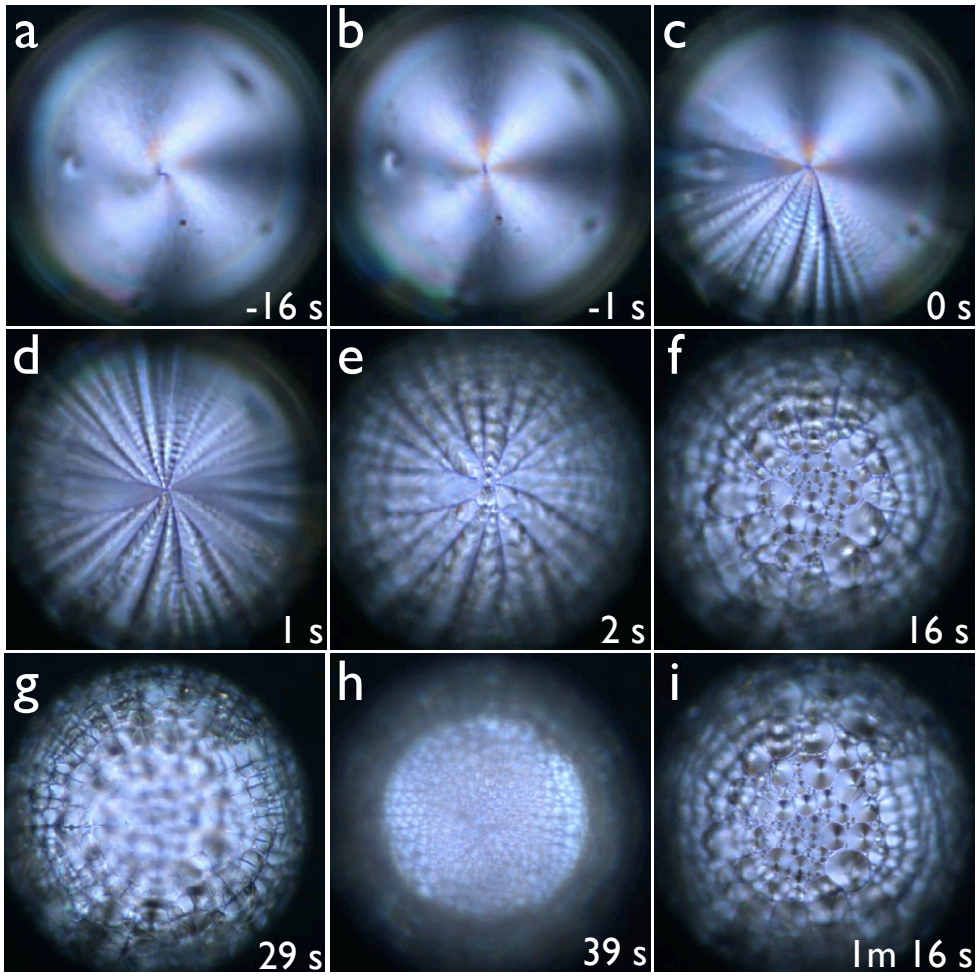

Figure 5. Nematic-Smectic-A transition on cooling an 8CB shell (about 340 μm diameter and about 18 μm thickness) with planar alignment on the outside and homeotropic on the inside. The time indications in each photo refer to the time before (negative times) or after the N-SmA transition. All photos except (h) are focused on the front side of the shell, whereas (h) is focused on the back (hence the smaller size).

combinations of these types in our recent paper [48], which we refer to for full details. Another example is shown in Fig. 5. In the nematic phase a bend deformation of the director field connects the homeotropic and planar inner and outer boundaries (in the depicted shell the outside is planar and the inside homeotropic, but the reverse situation yields about the same results). This geometry is allowed in the nematic, as it is free of positional order, but it rules out the appearance of half-integer defects since the bend defines a direction in the shell plane that is not sign-invariant [48]. Consequently only two $s = +1$ defects are seen in the shell, one at the top (front in the direction of view in the microscope) and one at the bottom (back). Interestingly, the resulting configuration in the shell studied in Fig. 5 is a slightly twisted bipolar configuration as can be recognised in pane (a).

As the transition to the smectic phase is approached the director field is straightened out and the twist is expelled, cf. Fig. 5b, as is expected due to the divergence of the twist and bend elastic constants when the system enters the SmA phase. The transition is recognised by the appearance of stripes connecting the two poles, wrapping around the shell as a fan that is opened up, cf. panes c-d. These stripes can be understood as the top and bottom boundaries of a folding membrane of remaining nematic order [48], connecting the smectic phases with opposite alignments at the top and bottom, as initially explained by Cladis and Torza for flat hybrid samples [51]. Since director bend is not allowed in the SmA phase the bend required for continuity is initially suppressed into these narrow regions of remaining nematic order, but very soon the nematic phase is fully expelled and then the stripes become unstable, following a Rayleigh instability break-up into domains with more or less circular cross section, cf. Fig. 5e-f. These domains are toric focal conic domains, within which the layers bend, thereby accommodating the opposing boundary conditions with no other director deformation than splay [48], allowed in SmA. Fig. 5f and i show these domains with focus at the top of the shell, whereas pane (g) is focused slightly lower and pane (h) is focused roughly on the shell bottom.

(*d*) *SmC shells and the SmA-SmC transition*

Our latest focus is on homeotropic-aligned shells exhibiting a SmA-SmC transition. This is an interesting situation since the smectic layers can be self-closing and dislocation-free if the shell is perfectly symmetric, hence the smectic order promotes shell symmetry and thus to some extent opposes the tendency to varying shell thickness driven by density mismatch or even by the extension of director field defects in planar-aligned nematic shells [37]. At the same time, the tilt in the SmC phase provides a tangential director field, thus giving rise to topological defects also in this configuration, in contrast to N and SmA phases which are defect-free in fully homeotropic alignment.

The tangential director field of SmC and its analogs (SmC_a etc.) is often referred to as the c-director field $\mathbf{c}$, and it is defined as the projection of the actual director $\mathbf{n}$ onto the smectic layer plane. As in case of hybrid alignment the c-director field of SmC-type phases is not sign invariant, meaning that only integer defects are allowed [52]. Thus, in a regular SmC phase without any inclusions we can normally expect no more than two defects per shell interface. However, in the SmC_a phase the sign invariance is reestablished through the possibility

of dispirations [53], a special type of defect allowed by the anticlinic tilting arrangement that is the hallmark of this smectic-C-type phase. In a shell made from this phase we can thus again expect four defects per shell interface, although the alignment is fully homeotropic as induced by standard ionic surfactants. This has the advantage that we can expect a particularly stable and symmetric shell, since ionic surfactants are among the best stabilisers of the interfaces between the liquid crystal and the aqueous phase, and since (as discussed above) the smectic layers developing in the spherical shell plane promote a central position of the internal droplet in order to allow self-closing of the layers. Since SmC_a often follows (in those substances that exhibit the SmC_a phase [54]) upon cooling from SmC, which in turn typically develops on cooling from SmA, we should, with a suitable smectic liquid crystal material building up the shell, be able to tune the number of defects per interface from 0 to 2 to 4 just by cooling. This could provide a very interesting dynamic system both for fundamental studies and for applications in smart colloids.

As a first convenient system for studying the SmC phase in shell configuration we have chosen a binary mixture of the similar smectogens 2-(4-hexyloxyphenyl)-5-octylpyrimidine and 2-(4-octyloxyphenyl)-5-octylpyrimidine at 50/50 mass ratio. This mixture exhibits a room temperature SmC phase and an SmA-SmC transition at 49.7°C which we initially thought was second order based on DSC investigations and observations in standard liquid crystal microscopy samples. Still images from a video showing the textural development upon cooling in a shell made of this mixture are shown in Fig. 6. While filming this video we found that the SmA-SmC transition in the mixture is in fact very weakly first order, because at the transition there is a sudden jump of the texture, clearly detectable although very small. In Fig. 6a-b we have drawn a thin green cross as guide for the eye to make this jump easier to spot. Pane (a) shows the shell as it is still in the SmA phase whereas pane (b) shows the first video frame after the transition. The conoscopy cross has jumped very slightly to the left and downwards at the transition. This suggests that texture observations of shells could be an interesting method of distinguishing extremely weakly first order phase transitions from true second order transitions.

As the shell is cooled deeper into the SmC phase the biaxiality of this phase gradually becomes apparent, but a rather complex distortion of the texture makes it difficult to analyse the director field. While it is very clear that the phase is no longer SmA it is not easy to spot the defects which ought to be present. The highly distorted texture may be due to the lack of correlation between the c-director on the front and back of the shell, leading to overlaid birefringence in an uncontrolled manner, as discussed initially in this paper. After some ten minutes a texture has developed that to some extent resembles a conoscopy texture of a biaxially birefringent material observed with circular polarised light. The microscope illumination is however still linear but it could be that the back side of the shell, not currently in focus, acts to some extent as a $\lambda/4$ plate and changes the polarisation to highly elliptical. Our inability to identify the defects may be due to the complex distorted c-director field, coupled to the fact that light scattering from a c-director defect may be less intense than from a nematic director field defect. On the other hand, it might also suggest that the defects are in fact not present: the liquid crystal could avoid the defects by locally reducing

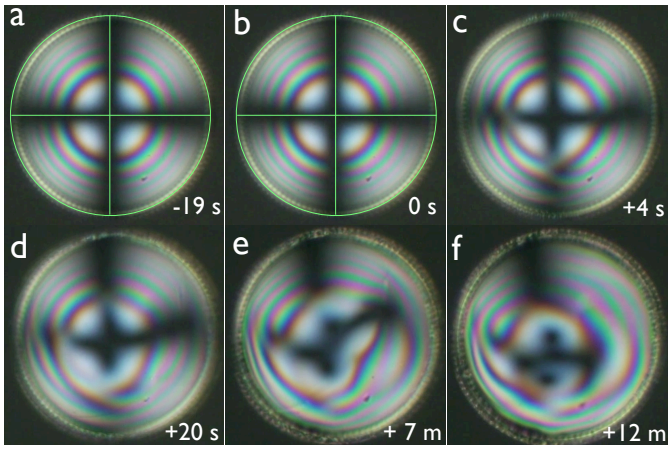

Figure 6. SmA-SmC transition on cooling a shell formed by a binary phenylpyrimidine mixture with homeotropic alignment on the in- and outside. The time indications in each photo refer to the time before (negative times) or after the SmA-SmC transition. The green cross in (a) and (b) is a guide for the eye to facilitate the detection of the tiny shift of the conoscopy cross occurring at the phase transition.

the tilt to zero, shifting the system to an SmA state in the 'defect point'. Further investigations, particularly with high-tilt materials, can hopefully help to elucidate this question.

(*e*) *Adding particles for further tuning of the defect configuration*

As mentioned above the introduction of defect-seeding particles into the shell may be an interesting way to further tune the number and type of defects. Controlled particle introduction of this type has so far not been explored in shells but we have seen that this in principle works, based on dust particles that were introduced by mistake into shells. This was particularly useful for SmC shells which, as just described, do not necessarily show any easily visible defects in their pristine state.

Fig. 7 shows two frames from a video of a SmC shell of the same mixture as discussed above, between crossed polarisers on the left and without analyser on the right. A few dust particles were collected at one point of the shell, a bit to the right of the centre of the picture, which can clearly be seen in the non-polarising image. Looking at the polarised image it is clear that defects in the c-director field have indeed been seeded at the particles, leading to distinct *schlieren* around the particles, although the texture is still not as easy to analyse as in case of nematic shells. In any case, this observation indicates that particles can seed defects, and they can be anchored in defects, even in SmC-type shells. This is promising for the future.

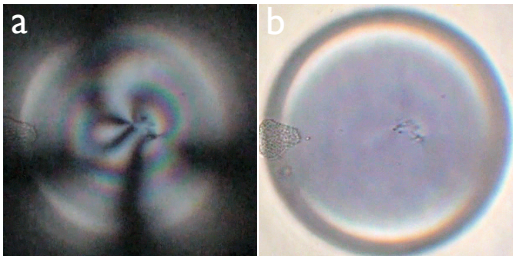

Figure 7. An SmC shell with a few dust particles slightly to the right of the centre in the image, viewed between crossed polarisers (a) and without analyser (b). The feature on the left is not part of the shell but an aggregate of some kind suspended in the continuous phase. For clarity the photos have been slightly enhanced digitally (increased exposure in both photos and increased contrast in the right one).

(*f*) *Outlook*

The study of liquid crystalline shells is still in its infancy, pursued only by a handful of groups around the world. While the initial focus was entirely on nematic shells, investigations of smectic shells have recently appeared. Already the very simplest SmA phase leads to very interesting and quite complex textural features and novel defect configurations, and the first preliminary observations of SmC phases hint at quite different behaviour. The additional degrees of freedom offered by the appearance of the c-director field open interesting possibilities, in particular when considering the multiple variations of smectic-C-type order that are available.

Moreover, it will be very interesting to study transitions to smectic phases with partial in-plane positional order, such as SmI, SmB or SmF. One may well expect visible effects on the shape of the shell due to the considerable stiffening of the liquid crystal upon such a transition, as previously seen in phospholipid vesicles undergoing an L_α-L_β' transition with a consequent strong faceting occurring [55]. Alternatively, the shell may even become unstable and break, as was observed in a very interesting case of vesicles undergoing the same L_α-L_β' phase transition but using a special type of synthetic phospholipid [56, 57]. In this case there was no faceting observed but instead the spherical vesicles were essentially 'dissolved' and replaced by a multiplicity of helical spirals which eventually merged into tubules. While a similar shape change is unlikely in case of thermotropic liquid crystal shells, since their interfaces with the aqueous phases need to be stabilised by surfactants or polymers, the observation that a spherical shell becomes unstable and collapses (most likely into a drop) may still shed light on the analogous process giving rise to the shape transition in the phospholipids, a phenomenon that is still not fully understood.

3. Liquid crystal-functionalised electrospun nano-/microfibres

(*a*) *Motivation: why study liquid crystals inside micro-/nanofibres?*

The main motivation for developing this new type of liquid crystal sample is the different application possibilities arising. The non-woven fibre mat produced by electrospinning is flexible, soft and light-weight and its high porosity gives it good breathability, allowing it to be incorporated into textile garments. By including a liquid crystal inside the fibres making up the mat we can thus bring the responsiveness and useful optical properties of liquid crystal into a new type of flexible and eventually wearable device. We are currently focusing primarily on the possibility to use the liquid crystal-functionalised mats as gas sensors, relying on the sensitive response of liquid crystals to the diffusion of gases [58–60], to be incorporated into garments, but many other application possibilities can be envisaged [61].

On the other hand, the strong cylindrical confinement inside the fibre can have considerable impact on the liquid crystal. In the following brief discussion we focus on this issue. Although the first example of liquid crystals confined in electrospun fibres was presented only in 2008 [62], the general issue of confinement effects on liquid crystals is a topic that has received much attention in the research community, and it continues to do so today. It is interesting to compare the electrospun fibres with the most commonly studied confining systems.

- *Planar plate confinement*
  The simplest way of studying liquid crystal confinement effects is to fill it between two flat glass substrates, i.e. using standard sample cells. Such studies have shown that even the relatively weak confinement resulting from parallel plates with a spacing in the micron range can dramatically change the phase sequence of e.g. chiral smectic liquid crystals [63–65] and/or it can stabilise structures different from the bulk structure, as in the case of surface-stabilised ferroelectric liquid crystals [66] where the helix is expelled by means of confinement. It is technically difficult to realise planar sample cells with nanometer scale substrate spacing but simulations of a liquid crystal that in bulk exhibits an isotropic-nematic-smectic sequence confined in a flat slab of 8 nm thickness revealed an increased degree of order, both orientational and translational [67]. In another simulation work [68] the structure of a twisted nematic cell was investigated as the substrate spacing was reduced towards zero, revealing a dramatic change upon reducing the spacing to some ten molecular lengths (about 30 nm), again a spacing which is challenging to realise in practice with standard cells.

- *Glass capillaries*
  The simplest way of studying cylindrical confinement is to fill the liquid crystal in a standard glass capillary. Surface anchoring can relatively easily be switched between planar and homeotropic by using different coatings of the inner glass surface, although a specific planar alignment direction (e.g. along or perpendicular to the capillary axis) is challenging to achieve. As for the standard flat cells the degree of confinement is however limited to the micron range, since glass capillaries are generally relatively thick. In fact,

the strongest confinement studied using glass capillaries was on the order of tens of microns [69].

- *Anopore and Nucleopore/Millipore membranes*
  Two systems that do provide cylindrical confinement in the nanoscale are Anopore (aluminum oxide, most common pore diameter 200 nm, length 60 μm [70]) and Nucleopore/Millipore (typically polycarbonate, pore diameter in the range 0.1-20 μm, length 10 μm [70, 71]) membranes. The raw surface of the latter has been reported not to enforce any preferred local alignment of liquid crystals [72], while that of Anopore should impose planar axial alignment [73]. In both cases the pore insides can be coated with selected materials, promoting planar or homeotropic surface anchoring [70], but confinement in 200 nm Anopore cylinder pores resulted in planar alignment along the cylinder axis even when the internal pore surface was coated for homeotropic anchoring [74]. This suggests that the elastic energies in submicrometer channels can overwhelm surface anchoring effects if these are not very strong. The director is aligned along the channel since this leads to a defect- and distortion-free director configuration. Most published studies of liquid crystals in these membranes have focused on extremely small diameters, on the orders of some tens of nanometers up to 100 or 200 nm. Among the key findings are surface-induced orientational order at temperatures well above the bulk isotropic-nematic transition temperature [74], connected to the replacement of the sharp first-order character of the transition by a continuous transition. It was also found to be shifted to lower temperatures in the confined system [75, 76]. Also the N-SmA transition of 8CB was found to be strongly affected inside 200 nm Anopore membrane pores, with a dramatic suppression of the specific heat and a slight shift to lower temperatures [75, 76]. Simulations of a liquid crystal confined in very thin cylindrical pores (diameter about 10 nm) with planar surface anchoring suggested that positional ordering was strongly inhibited, counteracting a transition from a nematic to a smectic phase [77].

- *Aerogels, aerosils, Vycor and Controlled-Pore Glass (CPG)*
  Another popular approach to study liquid crystal confinement effects is to include the liquid crystal inside random porous matrices, imposing a *disordering* influence on the director field. Aerogels are formed by gelation of 3- to 5 nm diameter silica particles, resulting in pores that curve strongly in random ways. The nanoparticles fuse from solution into fractal clusters, forming an inorganic network that is stabilised by covalent bonds, yielding a rigid highly porous structure with silica volume fraction down to 0.05 and a typical cavity dimension in the range 10 to 100 nm [78]. Aerosils are also based on silica particles, but here they are dispersed directly in the liquid crystal, allowing gelation to occur afterwards. The random silica network that forms is rather loosely kept together through interparticle hydrogen bonds, and it may thus break up and rearrange on moderate time scales to relieve strains imposed by the contained liquid crystal, provided that the silica concentration is not too high [72]. Vycor and CPG are two commercial porous glass types, also consisting of a random porous 3D-interconnected SiO_2 network, albeit produced via different routes. Several studies using

these types of matrix have provided data for extremely small confinement (pore size down to 7 nm) [79, 80].

- *Ordered porous alumina templates*
  Similar to Anopore, these templates provide confinement in parallel non-connected straight cylinders, but the pores are arranged with high spatial periodicity. Steinhart and co-workers studied the alignment of discotic liquid crystals in ordered porous alumina templates with pore diameters of 400 and 60 nm, respectively, and a pore length of 100 μm, either directly [81] or after first coating the pore walls with a layer of poly(methyl methacrylate (PMMA) [82].

The electrospun fibres can be compared to other confining systems where the surfaces impose planar alignment, because so far planar anchoring was found in all fibres. With other (rather special) sheath polymers or with careful addition of surfactants into the sheath mixture it might be possible to induce homeotropic anchoring, although the above mentioned studies indicate that the confinement will most likely still impose alignment along the fibre for core diameters below several 100 nm. A major difference from the random porous structures is that the disordering effect is generally not expected in the case of electrospun fibres, as they can provide confinement in very long cylinders (disregarding the case of fibres with strong break-up of the core fluid, which is generally not desired).

One advantage with the electrospun fibres compared to the alternative methods is that no filling step is involved. The fibres are produced with the liquid crystal included from the start. Since filling of a matrix with sub-micron pores is typically a very slow process, potentially with problems caused by air bubbles (unless the filling is done in vacuum) this can be a valuable aspect. On the other hand, if the spinning conditions are not right then the liquid crystal stream is broken up into droplets and there is no way to change this after spinning. Another highly beneficial aspect of the electrospinning approach to studying confinement is that the fibre sheath, in contrast to many of the alternative confining matrices, can be optically transparent and the light scattering can be kept within acceptable limits [83,84]. This allows for optical methods, in particular polarising microscopy, for studying the impact of confinement on the liquid crystal.

(*b*) *Production of liquid crystal-core microfibres*

In electrospinning the fluid(s) to be spun is (are) pumped gently through a spinneret, connected to a high voltage power supply and mounted some 10-20 cm from a grounded collector electrode, cf. Fig. 8. The power supply charges the fluid in contact with the electrode to the extent that the electrostatic forces overcome the surface tension and a filament is ejected from the droplet that protrudes from the spinneret, and this is launched against the collector electrode. However, due to electrostatic self repulsion the jet path is not straight but highly spiraling, leading to a dramatic thinning of the filament before it reaches the collector. The fluid is typically a polymer solution, at a concentration selected such that the solvent will have evaporated almost completely by the time the filament hits the collector, thus producing a stable polymer fibre. By including a second capillary inside the spinneret—so-called coaxial electrospinning—we can introduce in principle any fluid we want inside the polymer sheath, since the polymer solution provides the

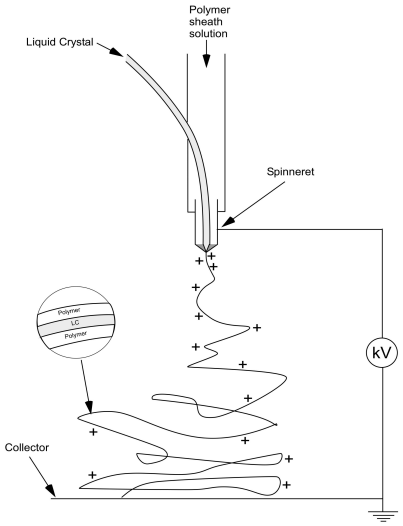

Figure 8. Schematic of the set-up used for coaxial electrospinning of core-sheath fibres with liquid crystal inside.

non-Newtonian properties required to prevent jet break-up into droplets via a Rayleigh instability.

This is the method we use to incorporate liquid crystals inside the fibre and it generally works very well, although the properties of the inner fluid and those of the polymer solution must fit to each other. First, they need to be immiscible to ensure a maintained coaxial fibre geometry [85]. Second, their elongational viscosity must be reasonably matched in order to avoid varicose break-up of the inner core into droplets [86]. With thermotropic liquid crystals as core fluid the first criterion calls for polymers soluble in polar solvents, and we therefore work primarily with polymers such as polyvinylpyrrolidone (PVP), polyvinylalcohol (PVA) or polyethyleneoxide (PEO). The molecular weight of the polymer should be high to ensure spinnability, typically in the range 1 million grams/mol, and the solvent should be volatile enough to evaporate almost completely during the jet's path from spinneret to collector. We often work with ethanol.

An alternative to the coaxial approach was developed by Buyuktanir et al. [87]. They simply mixed the polymer and the liquid crystal in a common solvent, relying on the phase separation between the low molar mass liquid crystal and the polymer upon solvent evaporation to produce the coaxial fibre. This leads to a remarkably simple approach to producing liquid crystal-functionalised electrospun fibres, although the control of the process and of the resulting fibre geometry is not quite as good as when using coaxial electrospinning.

(*c*) *Fibres with encapsulated N, SmA and SmC phases*

Our first experiments on liquid crystal electrospinning were done with a purely nematic commercial mixture, Roche RO-TN-403, in the core [62]. This first activity served to confirm that liquid crystal-functionalised polymer fibres could be fabricated in this way and to investigate the alignment of the director, which turned out to be along the fibre, as expected from the earlier confinement studies summarised above. More surprising was that the isotropic-nematic transition behaviour was dramatically changed, essentially resembling a second order transition and with traces of nematic order being detectable more than 20 K above the bulk transition temperature of the liquid crystal mixture used. Although we could not determine the core diameter of these first fibres we believe, based on related experiments with non-liquid crystalline core fluids as well as later experiments with liquid crystals done by us, that the cavity in which the liquid crystal was encapsulated was probably several hundred nanometers in diameter. This means that the very strong confinement employed by Crawford and co-workers [74], as mentioned above, to observe this type of change in the N-isotropic transition may not be necessary.

Later on we spun fibres with 8CB in the core [83], allowing us to study nematic as well as SmA phases and the transition between them in the fibres. Interestingly, in these fibres the effect on the isotropic-nematic transition was only marginal, and when there was a change it was rather in the opposite direction, i.e. a surface-induced weakening of liquid crystal order. This difference may be attributed to a slightly softer sheath (it was pure PVP while the earlier work was done with a PVP-TiO_2 composite sheath), a somewhat greater fibre diameter, or simply to the different liquid crystal materials used. As discussed further below, we believe the latter factor is the dominating one. The two most interesting observations from this study was first that the planar alignment was retained in the SmA phase, i.e. the smectic layers did not form concentrically as one might expect for cylindrical confinement but rather as 'slices' of tiny lateral extension oriented perpendicular to the fibre axis. This was confirmed by x-ray scattering experiments on samples with aligned fibres. This may on the one hand be due to the planar-aligning effect of the PVP sheath, on the other to the fact that the key flow process during spinning is one of extensional and not of shear flow, since the fibres are subject to extreme stretching during spinning. The anisotropy in extensional viscosity can be different from that in shear viscosity for the SmA phase.

Second, the N-SmA transition was often not detected during DSC investigations, at least in the thinner fibres. If a sample was heated to the isotropic phase and then cooled to room temperature, the nematic phase formed roughly at the same temperature as in bulk, but no sign of a transition to smectic was found. But if the sample was now left for a few weeks, the liquid crystal in the core had eventually transitioned entirely to SmA. This was verified by a DSC scan upon heating, in which the SmA-N transition was now easily detectable, albeit at somewhat increased temperature. Our interpretation [83] is that the surface-induced anchoring quite strongly retains whatever positional order is present in the liquid crystal. Upon cooling from nematic to SmA it thus takes very long for the mesogens to reorganize into the layered structure since the molecules at the interface to the polymer sheath are still positionally disordered. Conversely, when heating to nematic it takes longer than usual for the layered arrangement to

disappear due to the influence of the surface-anchored mesogens, explaining the shift in transition temperature. These observations match the results mentioned above by Qing et al. from simulations of the nematic-smectic transition under confinement [77].

Only recently we have begun spinning fibres with a material forming a SmC phase in the core. We used the same binary phenylpyrimidine mixture as used in the SmC shell production, showing a room temperature SmC phase and an SmC-SmA-N-iso phase sequence. Preliminary results from x-ray scattering investigations on aligned samples show that no shift in the SmA-SmC transition could be detected in these fibres and that the average molecule tilt in the SmC phase is similar to that of bulk samples. However, the director remains aligned along the fibre axis, which means that the layers must either be uniformly tilted within the fibres or folded into a cone-like structure.

(*d*) *Chiral nematics and blue phases encapsulated inside the fibre*

One of the most interesting systems studied so far inside the fibres was a chiral mixture that in bulk exhibits a room temperature cholesteric phase as well as a small temperature blue phase just below the isotropic phase. When examining the fibres with this liquid crystal [84] we again found a substantial increase of the clearing point, the extension of liquid crystalline order being 12°C for the thinnest fibres studied. These fibres were also pure PVP and the inner dimension did not go below a few hundred nanometers, but the mixture was based on the same Roche RO-TN-403 nematic as was used in the first study [62], where a considerable extension of liquid crystalline order was detected. This indicates that the effects of confinement indeed depend very much on the particular mesogens used.

Even more interesting was that no trace of the cholesteric-blue phase transition could be detected in these fibres, regardless of method used. Eventually we realised that this can be understood as an effect of the rather peculiar director geometry that is induced in the cholesteric phase due to the cylindrical encapsulation. Since the director is along the fibre axis at the interface to the sheath the cholesteric helix must develop radially. This means that we get selective reflection when observing the fibres perpendicular to the fibre direction, which is indeed what we found. However, it also means that the director adopts a 'double-twist cylinder' configuration, just as in the blue phase, only that here there is only one cylinder. Since the diameter of the core of the electrospun fibres is so small, the dimensions of the fibre-induced double-twist cylinder approaches that of a regular blue phase double-twist cylinder, meaning that the cholesteric and blue phases have become degenerate in the fibres [84]. It is thus no surprise that the transition between these two phases is absent in the fibre samples, since essentially nothing should change here. The situation would change in case of substantially thicker fibres and indeed we sometimes saw a more normal blue phase-like texture in some areas with very thick fibre diameter.

A curious behaviour was seen in a series of samples spun with sturdier sheaths, obtained either by increasing the polymer concentration or by adding a sol-gel precursor that gives composite sheaths with PVP and TiO_2. In this case the viscosities of the core and sheath fluids were not well matched, leading to break-up of the core fluid stream into droplets. The selective reflection could still be observed from the droplets in the fibres, as shown in Fig. 9. However, rather than

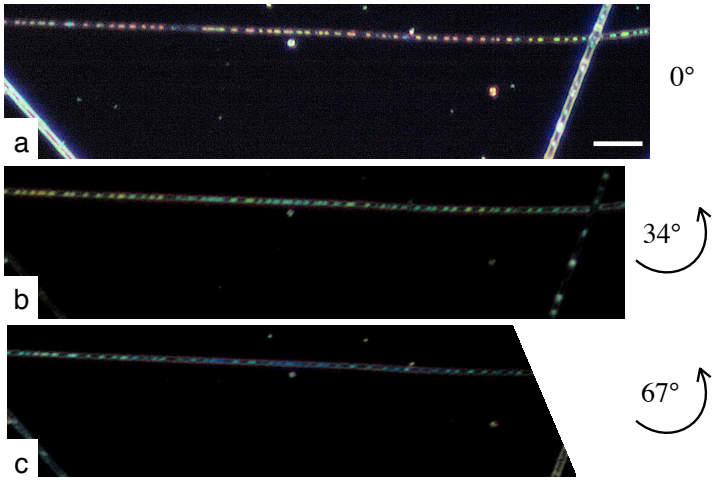

Figure 9. Reflection polarising microscopy images of a fibre with composite sheath consisting of 91% PVP and 9% TiO_2, and cholesteric core. The sample is pictured for three different sample orientations with respect to the crossed polarisers and the photos have been enhanced digitally (increased exposure) to make the colour variations easier to detect. The scale bar represents 10 μm.

giving an orientation independent reflected colour when illuminated by linearly polarised light, as for ordinary planar-aligned cholesterics and for all other fibres from which the liquid crystal gave selective reflection, the colour of the droplets in these fibres (as seen through the analyser) changed from blue to red if the sample was rotated (panes a-c). The origin of this phenomenon has not yet been clarified. It seems likely that the polarisation of the incoming light with respect to the director at the top of the liquid crystal droplet becomes important for samples as small as these.

(*e*) *Outlook: adding particles to the LC in the fibre core*

Just like with the thrust in producing and investigating liquid crystalline shells discussed above, the research field dealing with liquid crystal-functionalised electrospun fibres is very recent, leaving a vast number of possibilities open to explore. An obvious choice for the future is the extension to more complex liquid crystal phases, e.g. chiral smectic-C-type phases which normally develop a spontaneous polarisation, giving them ferro- or antiferroelectric properties. Another alternative, closer to the topic of this meeting, is to include particles in the liquid crystal, giving very interesting behaviour already for simple achiral nematics, as discussed above. The strong cylindrical encapsulation adds an additional constraint that can be quite interesting for the resulting structures, such that one could expect for instance chains of particles lining up along the core of the fibre. If the liquid crystal is heated to the isotropic phase the elastic forces acting on the particles disappears and the chains may dissolve. With conducting particles we could thus for instance imagine a temperature-controlled switching between percolation-induced conductivity along the fibres and no conductivity.

If we would use silica particles we would have a situation similar to an aerosil but now the gelation of the system would take place within a narrow cylindrical channel, most likely guiding the structures into a non-random arrangement. Many other phenomena can be contemplated, depending on what liquid crystal, which particles and what fibre diameter and sheath material is used.

4. Concluding remarks

This paper discusses our two recent research thrusts on liquid crystalline shells and electrospun polymer fibres functionalised by liquid crystal in the core. We have given a concise summary of our previous work, referring to the original articles for the details, as well as given some new preliminary data on SmC shells and on fibres with encapsulated cholesteric droplets. A special focus has been to place these two novel liquid crystal configurations in the context of particle – liquid crystal composites, where many interesting possibilities still remain to explore. In particular for liquid crystalline shells the introduction of particles may be a very rewarding way of controlling the defect configuration and the number of defects available for anchoring ligands, which in turn can lead to aggregation of the shells into colloidal crystals of variable symmetries. But also for the case of electrospun liquid crystal core fibres, included particles can provide an attractive variation possibility, as the particles are now confined within the narrow cylindrical space of the fibre core, yet they are surrounded by the liquid crystal which acts on them via the peculiar elastic forces and torques unique to this state of matter.

Acknowledgment

This work was financially supported by the German Academic Exchange Service DAAD, the "Excellenzcluster nanostrukturierte Materialien" (Sachsen-Anhalt, Germany), the Advanced Institutes of Convergence Technology (SNU, Korea) grant nr. 490- 20100024, Seoul National University grants nr. 490-20100021 and 490-20110040, and the National Research Foundation (Korea) grant nr. 490-20110016.

References

U. Tkalec, M. Ravnik, S. Copar, S. Zumer, and I. Musevic, "Reconfigurable knots and links in chiral nematic colloids," *Science*, vol. 333, no. 6038, pp. 62–65, 2011.

M. Skarabot and I. Musevic, "Direct observation of interaction of nanoparticles in a nematic liquid crystal," *Soft Matter*, vol. 6, no. 21, pp. 5476–5481, 2010.

I. Musevic, "Forces in nematic liquid crystals: from nanoscale interfacial forces to long-range forces in nematic colloids," *Liq. Cryst.*, vol. 36, no. 6-7, pp. 639–647, 2009.

U. Ognysta, A. Nych, V. Nazarenko, M. Skarabot, and I. Musevic, "Design of 2D binary colloidal crystals in a nematic liquid crystal," *Langmuir*, vol. 25, no. 20, pp. 12092–12100, 2009.

M. Conradi, M. Ravnik, M. Bele, M. Zorko, S. Zumer, and I. Musevic, "Janus nematic colloids," *Soft Matter*, vol. 5, no. 20, pp. 3905–3912, 2009.

U. Tkalec, M. Ravnik, S. Zumer, and I. Musevic, "Vortexlike topological defects in nematic colloids: Chiral colloidal dimers and 2D crystals," *Phys. Rev. Lett.*, vol. 103, no. 12, p. 127801, 2009.

M. Skarabot, M. Ravnik, S. Zumer, U. Tkalec, I. Poberaj, D. Babic, and I. Musevic, "Hierarchical self-assembly of nematic colloidal superstructures," *Phys. Rev. E*, vol. 77, no. 6, p. 061706, 2008.

U. Tkalec, M. Skarabot, and I. Musevic, "Interactions of micro-rods in a thin layer of a nematic liquid crystal," *Soft Matter*, vol. 4, no. 12, pp. 2402–2409, 2008.

I. Musevic and M. Skarabot, "Self-assembly of nematic colloids," *Soft Matter*, vol. 4, no. 2, pp. 195–199, 2008.

M. Ravnik, M. Skarabot, S. Zumer, U. Tkalec, I. Poberaj, D. Babic, N. Osterman, and I. Musevic, "Entangled nematic colloidal dimers and wires," *Phys. Rev. Lett.*, vol. 99, no. 24, p. 247801, 2007.

I. Musevic, M. Skarabot, U. Tkalec, M. Ravnik, and S. Zumer, "Two-dimensional nematic colloidal crystals self-assembled by topological defects," *Science*, vol. 313, no. 5789, pp. 954–958, 2006.

O. Mondain-monval and P. Poulin, "Mixed colloid-surfactant systems," *J. Phys.-Condens. Matter.*, vol. 16, no. 19, pp. S1873–S1885, 2004.

J. Loudet, P. Hanusse, and P. Poulin, "Stokes drag on a sphere in a nematic liquid crystal," *Science*, vol. 306, no. 5701, pp. 1525–1525, 2004.

J. Loudet, P. Barois, and P. Poulin, "Colloidal ordering from phase separation in a liquid-crystalline continuous phase," *Nature*, vol. 407, no. 6804, pp. 611–613, 2000.

M. Zapotocky, L. Ramos, P. Poulin, T. Lubensky, and D. A. Weitz, "Particle-stabilized defect gel in cholesteric liquid crystals," *Science*, vol. 283, pp. 209–212, 1999.

P. Poulin and D. A. Weitz, "Inverted and multiple nematic emulsions," *Phys. Rev. E*, vol. 57, no. 1, pp. 626–637, 1998.

P. Poulin, H. Stark, T. Lubensky, and D. A. Weitz, "Novel colloidal interactions in anisotropic fluids," *Science*, vol. 275, no. 5307, pp. 1770–1773, 1997.

H. Stark and D. Ventzki, "Stokes drag of spherical particles in a nematic environment at low ericksen numbers.," *Phys. Rev. E*, vol. 64, p. 031711, 2001.

H. Stark, "Director field configurations around a spherical particle in a nematic liquid crystal," *Eur. Phys. J. B*, vol. 10, no. 2, pp. 311–321, 1999.

P. Pishnyak, Oleg, V. Shiyanovskii, Sergij, and D. Lavrentovich, Oleg, "Inelastic collisions and anisotropic aggregation of particles in a ÂăÂănematic collider driven by backflow," *Phys. Rev. Lett.*, vol. 106, no. 4, p. 047801, 2011.

O. Pishnyak, S. Tang, J. Kelly, S. Shiyanovskii, and O. Lavrentovich, "Levitation, lift, and bidirectional motion of colloidal particles in an electrically driven nematic liquid crystal," *Phys. Rev. Lett.*, vol. 99, no. 12, p. 127802, 2007.

G. Liao, I. Smalyukh, J. Kelly, O. Lavrentovich, and A. Jákli, "Electrorotation of colloidal particles in liquid crystals," *Phys. Rev. E*, vol. 72, no. 3, p. 31704, 2005.

P. Petrov and E. M. Terentjev, "Formation of cellular solid in liquid crystal colloids," *Langmuir*, vol. 17, no. 10, pp. 2942–2949, 2001.

V. Anderson, E. M. Terentjev, S. P. Meeker, J. Crain, and W. C. K. Poon, "Cellular solid behaviour of liquid crystal colloids - 1. phase separation and morphology," *Eur. Phys. J. E*, vol. 4, no. 1, pp. 11–20, 2001.

V. Anderson and E. M. Terentjev, "Cellular solid behaviour of liquid crystal colloids - 2. mechanical properties," *Eur. Phys. J. E*, vol. 4, no. 1, pp. 21–28, 2001.

S. P. Meeker, W. C. K. Poon, J. Crain, and E. M. Terentjev, "Colloid-liquid-crystal composites: An unusual soft solid," *Phys. Rev. E*, vol. 61, no. 6, pp. R6083–R6086, 2000.

R. Ruhwandl and E. M. Terentjev, "Long-range forces and aggregation of colloid particles in a nematic liquid crystal," *Phys. Rev. E*, vol. 55, no. 3, pp. 2958–2961, 1997.

O. Kuksenok, R. Ruhwandl, S. Shiyanovskii, and E. M. Terentjev, "Director structure around a colloid particle suspended in a nematic liquid crystal," *Phys. Rev. E*, vol. 54, no. 5, pp. 5198–5203, 1996.

C. Bohley and R. Stannarius, "Inclusions in free standing smectic liquid crystal films," *Soft Matter*, vol. 4, no. 4, pp. 683–702, 2008.

C. Bohley and R. Stannarius, "Colloidal inclusions in smectic films with spontaneous bend," *Eur. Phys. J. E*, vol. 23, no. 1, pp. 25–30, 2007.
C. Bohley and R. Stannarius, "Energetics of 2d colloids in free-standing smectic-c films.," *Eur Phys J E Soft Matter*, vol. 20, no. 3, pp. 299–308, 2006.
H. Schuring and R. Stannarius, "Isotropic droplets in thin free standing smectic films," *Langmuir*, vol. 18, no. 25, pp. 9735–9743, 2002.
D. Nelson, "Toward a tetravalent chemistry of colloids," *Nano. Lett.*, vol. 2, no. 10, pp. 1125–1129, 2002.
M. Kleman and O. D. Lavrentovich, "Liquids with conics," *Liq. Cryst.*, vol. 36, no. 10-11, pp. 1085–1099, 2009.
M. Kleman and O. Lavrentovich, "Topological point defects in nematic liquid crystals," *Philosophical Magazine*, vol. 86, no. 25-26, pp. 4117–4137, 2006.
C. Blanc and M. Kleman, "The confinement of smectics with a strong anchoring," *Eur. Phys. J. E*, vol. 4, no. 2, pp. 241–251, 2001.
A. Fernandez-Nieves, V. Vitelli, A. Utada, D. R. Link, M. Marquez, D. R. Nelson, and D. A. Weitz, "Novel defect structures in nematic liquid crystal shells," *Phys. Rev. Lett.*, vol. 99, no. 15, p. 157801, 2007.
T. Lopez-Leon, V. Koning, K. B. S. Devaiah, V. Vitelli, and A. Fernandez-Nieves, "Frustrated nematic order in spherical geometries," *Nat. Phys.*, vol. 7, pp. 391–394, 2011.
T. Lopez-Leon and A. Fernandez-Nieves, "Drops and shells of liquid crystal," *Colloid Polym. Sci.*, vol. 289, no. 4, pp. 345–359, 2011.
M. Maldovan, C. Ullal, W. Carter, and E. Thomas, "Exploring for 3D photonic bandgap structures in the 11 f.c.c. space groups.," *Nat. Mater.*, vol. 2, no. 10, pp. 664–667, 2003.
A. Hynninen, J. Thijssen, E. Vermolen, M. Dijkstra, and A. van Blaaderen, "Self-assembly route for photonic crystals with a bandgap in the visible region.," *Nat. Mater.*, vol. 6, no. 3, pp. 202–205, 2007.
S. Samitsu, Y. Takanishi, and J. Yamamoto, "Molecular manipulator driven by spatial variation of liquid-crystalline order.," *Nat. Mater.*, vol. 9, no. 10, pp. 816–820, 2010.
J. P. F. Lagerwall and G. Scalia, "A new era for liquid crystal research: Applications of liquid crystals in soft matter nano-, bio- and microtechnology," *Current Applied Physics*, vol. 12, 2012.
A. Utada, E. Lorenceau, D. R. Link, P. D. Kaplan, H. A. Stone, and D. A. Weitz, "Monodisperse double emulsions generated from a microcapillary device," *Science*, vol. 308, no. 5721, pp. 537–541, 2005.
H.-L. Liang, E. Enz, G. Scalia, and J. Lagerwall, "Liquid crystals in novel geometries prepared by microfluidics and electrospinning," *Mol. Cryst. Liq. Cryst.*, vol. 549, pp. 69–77, 2011.
S. Sivakumar, L. Wark, Kim, K. Gupta, Jugal, L. Abbott, Nicholas, and F. Caruso, "Liquid crystal emulsions as the basis of biological sensors for the optical detection of bacteria and viruses," *Adv. Funct. Mater.*, vol. 19, no. 14, pp. 2260–2265, 2009.
H.-L. Liang, S. Schymura, P. Rudquist, and J. Lagerwall, "Nematic-smectic transition under confinement in liquid crystalline colloidal shells," *Phys. Rev. Lett.*, vol. 106, no. 24, p. 247801, 2011.
H.-L. Liang, R. Zentel, P. Rudquist, and J. Lagerwall, "Towards tunable defect arrangements in smectic liquid crystal shells utilizing the nematic-smectic transition in hybrid-aligned geometries," *Soft Matter*, vol. 8, no. 20, pp. 5443–5450, 2012.
T. Lopez-Leon, A. Fernandez-Nieves, M. Nobili, and C. Blanc, "Nematic-smectic transition in spherical shells," *Phys. Rev. Lett.*, vol. 106, no. 24, p. 247802, 2011.
H. Shin, M. Bowick, and X. Xing, "Topological defects in spherical nematics," *Phys. Rev. Lett.*, vol. 101, no. 3, p. 037802, 2008.
P. Cladis and S. Torza, "Growth of a smectic-a from a bent nematic phase and smectic light valve," *J. Appl. Phys.*, vol. 46, no. 2, pp. 584–599, 1975.
P.-G. de Gennes and J. Prost, *The physics of liquid crystals.*
Oxford, UK: Clarendon Press, 1993.

Y. Takanishi, H. Takezoe, a. Fukuda, and J. Watanabe, "Visual observations of dispirations in liquid crystals," *Phys. Rev. B*, vol. 45, no. 14, pp. 7684–7689, 1992.

J. P. F. Lagerwall and F. Giesselmann, "Current topics in smectic liquid crystal research," *ChemPhysChem*, vol. 7, no. 1, pp. 20–45, 2006.

M. Andersson, L. Hammarstrom, and K. Edwards, "Effect of bilayer phase-transitions on vesicle structure and its influence on the kinetics of viologen reduction," *J. Phys. Chem.*, vol. 99, no. 39, pp. 14531–14538, 1995.

J. Selinger, M. Spector, and J. Schnur, "Theory of self-assembled tubules and helical ribbons," *J. Phys. Chem. B*, vol. 105, no. 30, pp. 7157–7169, 2001.

J. Schnur, B. Ratna, J. Selinger, a. Singh, G. Jyothi, and K. Easwaran, "Diacetylenic lipid tubules - experimental-evidence for a chiral molecular architecture," *Science*, vol. 264, no. 5161, pp. 945–947, 1994.

Y. Han, K. Pacheco, C. W. M. Bastiaansen, D. J. Broer, and R. P. Sijbesma, "Optical monitoring of gases with cholesteric liquid crystals," *J. Am. Chem. Soc.*, vol. 132, no. 9, pp. 2961–2967, 2010.

A. Mujahid, H. Stathopulos, A. Lieberzeit, Peter, and L. Dickert, Franz, "Solvent vapour detection with cholesteric liquid crystals-optical and mass-sensitive evaluation of the sensor mechanism," *Sensors*, vol. 10, no. 5, pp. 4887–4897, 2010.

C.-K. Chang, H.-L. Kuo, K.-T. Tang, and S.-W. Chiu, "Optical detection of organic vapors using cholesteric liquid crystals," *Appl. Phys. Lett.*, vol. 99, no. 7, p. 073504, 2011.

J. P. F. Lagerwall, "Three facets of modern liquid crystal science," *Habilitation thesis, Martin-Luther-Universität Halle-Wittenberg*, 2010.

J. P. F. Lagerwall, J. T. McCann, E. Formo, G. Scalia, and Y. Xia, "Coaxial electrospinning of microfibres with liquid crystal in the core," *Chem. Commun.*, no. 42, pp. 5420–5422, 2008.

M. Skarabot, S. Kralj, R. Blinc, and I. Musevic, "The smectic a-smectic c* phase transition in submicron confined geometry," *Liq. Cryst.*, vol. 26, no. 5, pp. 723–729, 1999.

J. P. F. Lagerwall, D. D. Parghi, D. Krüerke, F. Gouda, and P. Jägemalm, "Phases, phase transitions and confinement effects in a series of antiferroelectric liquid crystals," *Liq. Cryst.*, vol. 29, no. 2, pp. 163–178, 2002.

M. Skarabot, R. Blinc, G. Heppke, and I. Musevic, "Electro-optic response of an antiferroelectric liquid crystal in submicron cells," *Liq. Cryst.*, vol. 28, no. 4, pp. 607–613, 2001.

N. A. Clark and S. T. Lagerwall, "Submicrosecond bistable electro-optic switching in liquid crystals," *Appl. Phys. Lett.*, vol. 36, no. 11, pp. 899–901, 1980.

Q. Ji, R. Lefort, and D. Morineau, "Influence of pore shape on the structure of a nanoconfined gay-berne liquid crystal," *Chem. Phys. Lett.*, vol. 478, no. 4-6, pp. 161–165, 2009.

L. Mirantsev and E. Virga, "Molecular dynamics simulation of a nanoscopic nematic twist cell," *Phys. Rev. E*, vol. 76, no. 2, p. 021703, 2007.

H. Kitzerow, B. Liu, F. Xu, and P. Crooker, "Effect of chirality on liquid crystals in capillary tubes with parallel and perpendicular anchoring," *Phys. Rev. E*, vol. 54, no. 1, pp. 568–575, 1996.

G. Crawford, L. Steele, R. Ondriscrawford, G. Iannacchione, C. Yeager, J. Doane, and D. Finotello, "Characterization of the cylindrical cavities of anopore and nucleopore membranes," *J. Chem. Phys.*, vol. 96, no. 10, pp. 7788–7796, 1992.

M. Kuzma and M. Labes, "Liquid crystals in cylindrical pores: effects on transition temperatures and singularities," *Mol. Cryst. Liq. Cryst.*, vol. 100, no. 1, pp. 103–110, 1983.

U. Zammit, M. Marinelli, F. Mercuri, and S. Paoloni, "Effect of confinement and strain on the specific heat and latent heat over the nematic-isotropic phase transition of 8CB liquid crystal," *J. Phys. Chem. B*, vol. 113, no. 43, pp. 14315–14322, 2009.

T. Jin, B. Zalar, A. Lebar, M. Vilfan, S. Zumer, and D. Finotello, "Anchoring and structural transitions as a function of molecular length in confined liquid crystals," *Eur. Phys. J. E*, vol. 16, pp. 159–165, 2005.

G. Crawford, R. Stannarius, and J. Doane, "Surface-induced orientational order in the isotropic-phase of a liquid-crystal material," *Phys. Rev. A*, vol. 44, no. 4, pp. 2558–2569, 1991.

G. Iannacchione and D. Finotello, "Calorimetric study of phase-transitions in confined liquid-crystals," *Phys. Rev. Lett.*, vol. 69, no. 14, pp. 2094–2097, 1992.

G. Iannacchione and D. Finotello, "Confinement and orientational study at liquid-crystal phase-transitions," *Liq. Cryst.*, vol. 14, no. 4, pp. 1135–1142, 1993.

J. Qing, R. Lefort, R. Busselez, and D. Morineau, "Structure and dynamics of a gay-berne liquid crystal confined in cylindrical nanopores," *J. Chem. Phys.*, vol. 130, no. 23, p. 234501, 2009.

T. Bellini, L. Radzihovsky, J. Toner, and N. Clark, "Universality and scaling in the disordering of a smectic liquid crystal," *Science*, vol. 294, no. 5544, pp. 1074–1079, 2001.

G. Iannacchione, G. Crawford, S. Qian, J. Doane, and D. Finotello, "Nematic ordering in highly restrictive vycor glass," *Phys. Rev. E*, vol. 53, no. 3, pp. 2402–2411, 1996.

G. Cordoyiannis, A. Zidansek, G. Lahajnar, Z. Kutnjak, H. Amenitsch, G. Nounesis, and S. Kralj, "Influence of confinement in controlled-pore glass on the layer spacing of smectic-a liquid crystals," *Phys. Rev. E*, vol. 79, no. 5, p. 051703, 2009.

M. Steinhart, S. Zimmermann, P. Göring, A. Schaper, U. Gösele, C. Weder, and J. Wendorff, "Liquid crystalline nanowires in porous alumina: Geometric confinement versus influence of pore walls," *Nano. Lett.*, vol. 5, no. 3, pp. 429–434, 2005.

M. Steinhart, S. Murano, A. Schaper, T. Ogawa, M. Tsuji, U. Gosele, C. Weder, and J. Wendorff, "Morphology of polymer/liquid-crystal nanotubes: Influence of confinement," *Adv. Funct. Mater.*, vol. 15, no. 10, pp. 1656–1664, 2005.

E. Enz, U. Baumeister, and J. Lagerwall, "Coaxial electrospinning of liquid crystal-containing poly(vinyl pyrrolidone) microfibers," *Beilstein J. Org. Chem.*, vol. 5, no. 58, p. DOI: 10.3762/bjoc.5.58, 2009.

E. Enz and J. Lagerwall, "Electrospun microfibres with temperature sensitive iridescence from encapsulated cholesteric liquid crystal," *J. Mater. Chem.*, vol. 20, no. 33, pp. 6866–6872, 2010.

D. Li and Y. Xia, "Direct fabrication of composite and ceramic hollow nanofibers by electrospinning," *Nano. Lett.*, vol. 4, no. 5, pp. 933–938, 2004.

J. McCann, M. Marquez, and Y. Xia, "Melt coaxial electrospinning: A versatile method for the encapsulation of solid materials and fabrication of phase change nanofibers," *Nano. Lett.*, vol. 6, no. 12, pp. 2868–2872, 2006.

A. Buyuktanir, Ebru, W. Frey, Margaret, and L. West, John, "Self-assembled, optically responsive nematic liquid crystal/polymer core-shell fibers: Formation and characterization," *Polymer*, vol. 51, no. 21, pp. 4823–4830, 2010.